UC Irvine
UC Irvine Previously Published Works

Title
Improving Bed Topography Mapping of Greenland Glaciers Using NASA's Oceans Melting Greenland (OMG) Data

Permalink
https://escholarship.org/uc/item/6vb3684g

Journal
Oceanography, 29(4)

ISSN
1042-8275

Authors
University of California, Irvine
Morlighem, Mathieu
Rignot, Eric
et al.

Publication Date
2016-12-01

DOI
10.5670/oceanog.2016.99

Peer reviewed

Improving Bed Topography Mapping of Greenland Glaciers Using NASA's Oceans Melting Greenland (OMG) Data

By Mathieu Morlighem, Eric Rignot, and Josh K. Willis

M/V *Cape Race* makes multibeam echosounding and conductivity-temperature-depth measurements in Uummannaq Fjord, West Greenland, in the summer of 2015 as part of NASA's Oceans Melting Greenland mission. *Photo credit: Christopher Kemp*

> 66 Glacier bed topography and bathymetry data are critical for better assessing the vulnerability of the Greenland Ice Sheet to climate change and improving projections of its future contribution to sea level rise. 99

ABSTRACT. Melting of the Greenland Ice Sheet has the potential to raise sea level by 7.36 m and is already contributing to global sea level rise at a rate higher than 1 mm yr^{-1}. Computer models are our best tools to make projections of the mass balance of Greenland over the next centuries, but these models rely on bed topography data that remain poorly constrained near glacier termini. Accurate bed topography in the vicinity of calving fronts is critical for numerical models, as the shapes of the glacier bed and of the nearby bathymetry control both the ocean circulation in the fjord and the stability and response of the ice sheet to climate warming. NASA's Oceans Melting Greenland (OMG) mission is collecting bathymetry data along Greenland fjords at several glacier termini. Here, we show that these measurements are transforming our knowledge of fjord and glacier depths. Using a mass conservation approach, we combine OMG bathymetry with observations of ice velocity and thickness to produce estimates of bed depth and ice thickness across the ice-ocean boundary with unprecedented accuracy and reliability. Our results along the northwest coast of Greenland reveal complex structural features in bed elevation, such as valleys, ridges, bumps, and hollows. These features have important implications for both channeling ice flow toward the continental margin, and for controlling the amount of warm, salty Atlantic Water that reaches the glaciers.

INTRODUCTION

The Greenland Ice Sheet has been losing mass in response to the rapid warming of the Arctic, and is contributing to sea level rise at an increasing rate (Rignot et al., 2011; Shepherd et al., 2012; Enderlin et al., 2014). Fluctuations in ocean and atmospheric circulations are not only affecting the amount of melting and run-off at the ice sheet surface, they are also contributing to the acceleration, thinning, and retreat of multiple outlet glaciers around Greenland (e.g., Howat et al., 2007; Moon et al., 2015; Mouginot et al., 2015). Complete melting of the Greenland Ice Sheet has the potential to raise sea level by 7.36 m. Already,

this melting is contributing more than 1 mm yr^{-1} of sea level rise, and the rate is increasing (Shepherd et al., 2012; Velicogna et al., 2014). Numerical models are the best tools for assessing the vulnerability of the Greenland Ice Sheet to climate warming and for making projections of the ice sheet under different CO_2 emission scenarios. Yet, predicting how fast the ice sheet will melt has proven to be challenging (Joughin et al., 2012), primarily because of our limited knowledge of bed topography and bathymetry in the vicinity of the ice sheet margin (Seroussi et al., 2011; Morlighem et al., 2014; Aschwanden et al., 2016).

Glacier bed topography and bathym-

etry data are critical for better assessing the vulnerability of the Greenland Ice Sheet to climate change and improving projections of its future contribution to sea level rise. Topography controls the stability of grounding lines (where grounded ice begins to float) and calving fronts of grounded glaciers (where icebergs break off from the glacier; e.g., Weertman, 1974; Schoof, 2007; Pattyn et al., 2013; Morlighem et al., 2016). For instance, it is well established that calving fronts and grounding lines are unstable on retrograde beds (i.e., the bed elevation becomes deeper below sea level going inland), except in the presence of high lateral shear (Gudmundsson et al., 2012). This phenomenon is known as marine ice sheet instability (MISI; Weertman, 1974) or tidewater instability (Post, 1975). Conversely, calving fronts of grounded glaciers and grounding lines are stabilized by topographic bumps or ridges in the bed that may slow down or even stop the retreat of glacier fronts. An accurate and precise knowledge of these features is therefore key to improving projections from numerical models.

Ice thickness and bed topography are routinely measured by airborne ice-penetrating radars that detect the ice/bed interface along profiles at a vertical resolution of approximately 50 m, depending on the radar wavelength (e.g., Evans and Robin, 1966; Gogineni et al., 1998). Yet, detecting the bed in coastal sectors,

where it matters most for ice sheet models, remains challenging. First, the highly crevassed surface of the ice near the coast creates signal scattering that generates clutter and noise. Second, the ice in these regions is often warm, and englacial water (water inside the glacier) attenuates the radar signal, potentially preventing it from reaching the bed. Finally, many of Greenland's marine-terminating glaciers flow along deeply entrenched valleys, and the signal echoes from adjacent bed topography (Holt et al., 2006). Despite major advances in radar sounding technology over the past two decades and a tripling of radar acquisitions with the advent of NASA's Operation IceBridge (OIB), major gaps in radar coverage remain along the coast of Greenland. Figure 1 shows the example of Store Gletscher in West Greenland. The black lines show the radar tracks from OIB where we have a positive identification of the bed (i.e., the ice/bed interface is clearly identifiable on radar echograms).

We see in Figure 1a that many of these black lines stop in the region of fast flow (in purple/red), indicating that the ice/bed interface is not detected by the radar. The bed topography under the ice stream, which controls the ice discharge of the entire basin, remains difficult to sound and poorly constrained. This problem is not specific to Store Gletscher; the depth of the bed of many ice streams along the periphery of the ice sheet is unknown. Figure 1b shows bed topography from Bamber et al. (2013) that relies on OIB measurements and a geostatistical technique called Kriging. Due to lack of data over the ice stream, the deep valley of Store Gletscher stops 8 km from the ice front, where the bed rises above sea level. This description of the bed topography is wrong because Store Gletscher is a marine-terminating glacier, and the ice bottom near the terminus is several hundreds of meters below sea level (Rignot et al., 2015). We cannot expect numerical models of ice sheet flow to be reliable in the periphery of the ice sheet with these data sets, which miss key features in bed topography.

A new method based on the conservation of mass (MC; Morlighem et al., 2011, 2013) has revolutionized ice thickness and bedrock mapping under the ice sheet (Aschwanden et al., 2016). Contrary to Kriging, MC does not rely solely on OIB measurements. It combines sparse ice thickness data with ice surface velocity data, for which we have complete coverage at high (150 m) resolution, and the principle of conservation of mass. This approach, described in more detail in the next section, has revealed that fjords and valleys extend further inland than previously thought, and remain below sea level for tens of kilometers (Morlighem et al., 2014). Figure 1c shows the MC-inferred bed topography of Store Gletscher 400 m below sea level at the glacier front, where the ice is in contact with the ocean. With MC, we map the bed topography of glaciers for which we have limited ice thickness observations, but these estimates remain poorly constrained by ice thickness measurements near glacier fronts, and errors in MC-inferred bed topography due to error in input data are potentially up to 100 m or more in some places. Thus, it is difficult to assess MC bed accuracy near glacier fronts. This problem of evaluation can be addressed by comparing the ice front depth from MC with measured bathymetry near the ice fronts.

Until today, bathymetry has remained largely unknown in the fjords of Greenland (Bamber et al., 2013). It has therefore been difficult to quantify the uncertainty in MC-derived bed topography near glacier fronts. Moreover, the lack
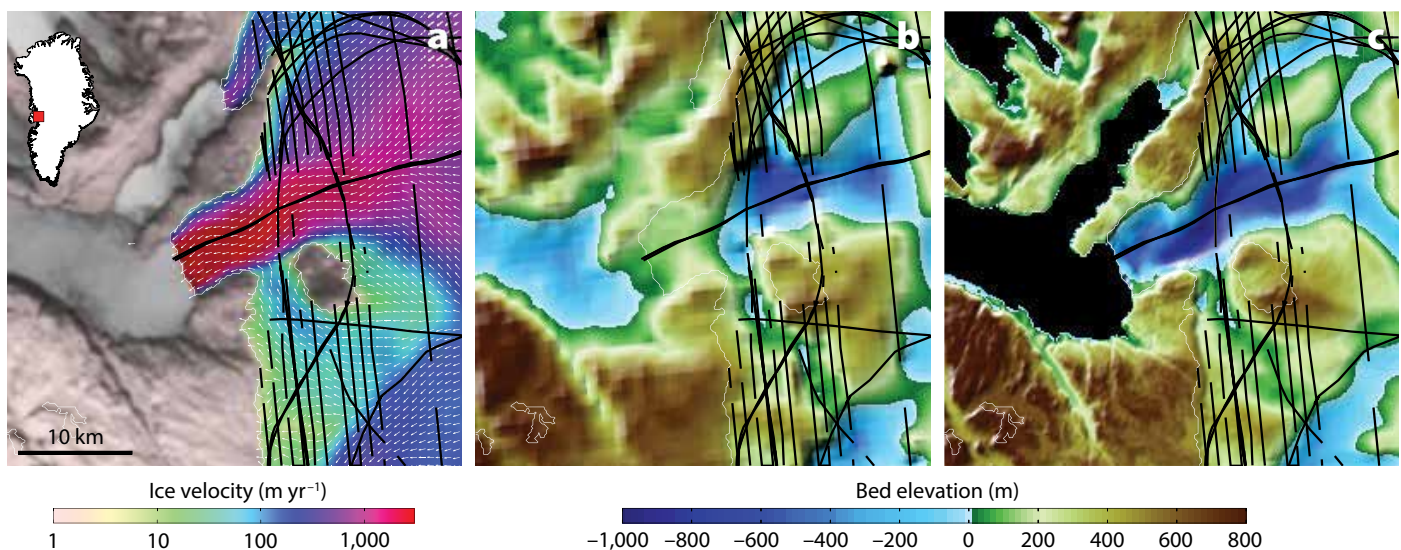

Figure 1. (a) Measured ice surface velocity of Store Gletscher, West Greenland (Rignot and Mouginot, 2012), overlaid on a Moderate Resolution Imaging Spectroradiometer (MODIS) Mosaic of Greenland (MOG). (b) Bed elevation from Bamber et al. (2013) color-coded between −1,000 m and +800 m, with areas below sea level in blue. (c) Bed elevation from Morlighem et al. (2014) using mass conservation. The white lines delineate the limit of land ice, and the black lines are Operation IceBridge (OIB) radar tracks with positive identification of the bed.

of bathymetry data precludes numerical modeling of ocean circulation within the fjord, which poses a fundamental limit on our understanding of ice-ocean interactions and how the Greenland Ice Sheet may respond to ocean warming.

One of the primary scientific objectives of NASA's Oceans Melting Greenland mission (OMG, https://omg.jpl.nasa.gov) is to improve our understanding of ocean circulation in the fjords and how this water interacts with Greenland's marine-terminating glaciers. Warm subsurface ocean waters of subtropical origin (Atlantic Water) are generally present below 200–250 m water depth in Greenland fjords, and these waters may or may not interact with the glacier termini, depending on the fjord's bathymetry; for example, the presence of a sill might block the ocean circulation at that depth and prevent this warm water from reaching the glacier front. Precise knowledge of the depth of these fjords is therefore needed to better understand which glaciers interact more strongly with the ocean and are more susceptible to enhanced ocean circulation in the fjords. Since 2015, OMG has been collecting a variety of data, including airborne gravity; high-resolution ice surface topography along the coast; conductivity, seawater temperature, and depth (CTD) from sensors deployed from boats and by air drop; and multibeam echosounding (MBES). Here, we only use MBES data that provide bathymetry at a horizontal resolution of 25 m with 1 m accuracy in fjords along the west coast of the Greenland Ice Sheet (OMG Mission, 2016a). We show that these measurements help constrain, and provide a means of evaluating, bed topography and ice thickness near the glacier fronts. Therefore, OMG bathymetry measurements not only improve the description of the fjords around the Greenland Ice Sheet, they also help improve our knowledge of the topography under the ice through a mass conservation approach. We apply this method along several glaciers of the northwest coast of Greenland.

DATA AND METHOD

The principle of mass conservation relies on a transport equation. For a given two-dimensional ice domain, Ω, if we know how much mass is coming along the inflow boundary Γ_- (i.e., its flux), and if we know where this ice is going and how much is added/subtracted locally (e.g., snow accumulation or ablation), MC determines the ice thickness over the entire ice domain by solving the mass conservation equation:

$$\begin{cases} \nabla \cdot H\overline{v} = \grave{a} \text{ in } \Omega \\ H = H_{obs} \text{ on } \Gamma_-, \end{cases} \quad (1)$$

where H is the ice thickness, $\overline{v}$ is the depth-averaged ice velocity vector, and $\grave{a}$ is the apparent mass balance (i.e., the sum of surface mass balance and thinning rate). To account for all OIB measurements of ice thickness, H_{obs}, along flight tracks, T, that lie within the model domain Ω, we formulate an optimization problem (Morlighem et al., 2011, 2013), where the following cost function must be minimized:

$$J(H) = \int_T \frac{1}{2}(H - H_{obs})^2 \, dT + R(H), \quad (2)$$

where R is a regularization term to avoid strong gradients in H. This minimization is under constraint as the ice thickness, H,

of the ice surface. We use the Greenland Ice Mapping Project Digital Elevation Model (GIMP DEM) from Howat et al. (2014) and apply this method to glaciers that are grounded at their termini. OMG is also collecting high-resolution (25 m) surface elevation data (OMG Mission, 2016b) along coastal Greenland, which could also be used to derive beds near glacier termini in the future.

We use ice velocity measurements derived from satellite radar data collected in 2008–2009 (Rignot and Mouginot, 2012) and assume that the surface velocity is a good approximation of the depth-averaged velocity for these fast flowing regions. The surface mass balance is averaged for the years 1961–1990 (Ettema et al., 2009), and ice thickening rates are from 2003–2008 from Schenk and Csatho (2012). We constrain the model by all OIB radar-derived thickness data. The inflow boundary follows a flight line of OIB for which we have good bed return, as it constrains all of the model downstream. There is a complete description of the mass conservation method in Morlighem et al. (2011). MC provides ice thickness and bed topography maps at a horizontal resolution of 150 m and a vertical accuracy of 50 m or higher depend-

> **" This new map, together with OMG temperature and salinity data from CTDs, opens the door to modeling ocean circulation in the entire fjord system in three dimensions, making it possible to better understand the vertical structure of ocean waters and its temporal variability. "**

is forced to satisfy the mass conservation equation (Equation 1). The bed topography under grounded ice is deduced by subtracting this mass-conserving ice thickness from a digital elevation model

ing on the spacing between flight lines and errors in input data: ice velocity, surface mass balance, and rate of ice thinning (Morlighem et al., 2013).

Here, we additionally use MBES

bathymetry data collected by OMG that have a horizontal resolution of 25 m and a vertical accuracy of 1 m (OMG Mission, 2016a). Integrating OMG bathymetry data with MC mapping is not straightforward, as OMG provides water depths in the vicinity of glacier termini and MC solves for ice thickness. Ocean depths must be translated into ice thicknesses at the ice front. The first step consists of looking for the closest bathymetry measurement for each point at the glacier terminus. The terminus position is given by the GIMP mask (Howat et al., 2014). If we find a bathymetry data point less than 100 m away, we assume that the depths at this point and at the calving face are the same, and deduce the ice thickness by adding this depth, $-b$, to the surface height above sea level given by the digital elevation model of the ice surface, s. This ice thickness at the calving front is then used in the optimization sequence of MC so that the modeled thickness is as close as possible to this prescribed thickness. MC indeed cannot impose ice thicknesses in any other place than the inflow boundary, Γ_-, but allows input parameters such as ice velocity or ice thinning rates to be adjusted within their respective error margins in order to minimize the cost function (Equation 2). We include an additional term to account for the OMG inferred ice thickness at the glacier front:

$$J(H) = \int_T \tfrac{1}{2}\,(H - H_{obs})^2\, dT +$$
$$\underbrace{\int_{terminus} \tfrac{1}{2}\,(H - (s - b))^2\, ds}_{\text{OMG constraint}} + R(H), \quad (3)$$

where s is the surface elevation from the GIMP DEM (Howat et al., 2014), and b is the OMG bathymetry. The benefit is that even though we might not have any radar-derived ice thickness constraint for tens of kilometers upstream, we now have one reliable and accurate constraint at the glacier terminus. Error in ice thickness from MC tends to increase along flow as we move away from ice thickness measurements that constrain the calculation. Without including OMG data at the ice front, errors in ice thickness are potentially large at the calving face, reaching 100 m or more. Integrating OMG data therefore has the potential to significantly reduce the error in bedrock elevation not only in the vicinity of glacier termini but also further upstream.

Figure 2 illustrates our methodology for Savissuaq WW and Savissuaq WWWW, following the naming convention of Rignot and Mouginot (2012), in Northwest Greenland. We first compile OMG bathymetry data and data for ice-free land (Figure 2a), then run MC by accounting for OIB and OMG data (Figure 2b), and fill data gaps in bathymetry (black areas in Figure 2) by relying on a natural neighbor algorithm.

We apply this method to the northwest coast of Greenland, where OMG has been collecting bathymetry data in previously uncharted waters, and compare our results to earlier maps from Bamber et al. (2013) and Morlighem et al. (2014) (Bedmachine Greenland) that did not include OMG data. Bamber et al. (2013) relied on the International Bathymetric Chart of the Arctic Ocean version 3 (IBCAOv3; Jakobsson et al., 2012). IBCAOv3 was a significant improvement over the previous version, but in a number of fjords, the bathymetry is unrealistically shallow, especially in narrow fjords where no bathymetry data were available prior to OMG. To overcome this issue, Bamber et al. (2013) manually lowered the bathymetry in the vicinity of some of these fjords.
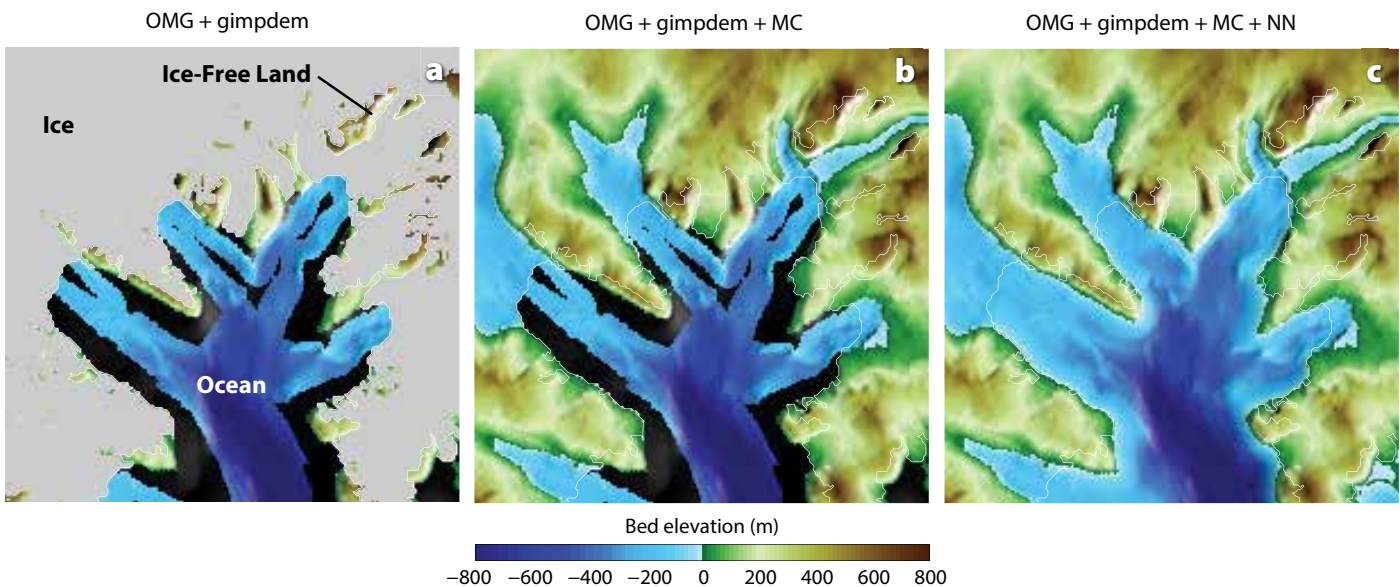
FIGURE 2. (a) OMG bathymetry (blue color scale) and ice-free land topography (green-brown color scale) from the Greenland Ice Mapping Project Digital Elevation Model (GIMP DEM; Howat et al., 2014) around Savissuaq WW, Northwest Greenland. The ice is shown in gray, and the black areas are the regions for which no bathymetry data are available. (b) Same map with integration of conservation of mass (MC) bed data. (c) Same map with natural-neighbor (NN) interpolation in the black area.

RESULTS AND DISCUSSION

Figure 3a shows the bed topography and ocean bathymetry of Savissuaq Gletscher before OMG from Bamber et al. (2013). Savissuaq Gletscher is a marine-terminating ice stream, about 5 km wide, located in Northwest Greenland (76.3°N, 65.6°W). The ocean bathymetry provided by Bamber et al. (2013) is flat and shallow (<100 m), rises near the ice front from 20 m below sea level to 50 m above sea level. According to this data set, Savissuaq Gletscher is a land-terminating glacier and does not interact with the ocean, which is incorrect. The topography of the bed under the ice shows a valley, close to sea level, that coincides with a flight line in the center of the ice stream and includes interpolation artifacts such as bumps and hollows typical of Kriging. Figure 3b shows the MC map before integrating OMG data (Bedmachine, Morlighem et al., 2014). MC uses the same radar measurements as those used by Bamber et al. (2013), but relies on mass conservation rather than Kriging. MC infers a well-defined valley that coincides with the ice stream but at a significantly higher resolution, and captures valleys under tributary glaciers that were missing in the previous map. While MC provides significant improvements over other mapping methods (Aschwanden et al., 2016), the bed at the glacier terminus is still between 0 m and 20 m above sea level, which is incorrect. The inclusion of OMG data at the glacier terminus mitigates this problem (Figure 3c). The new map shows a fjord that remains continuously below sea level for about 20 km upstream of the terminus, which lies 150 m below sea level at its deepest point. Without this additional constraint, MC was already able to capture important features in the bed, but the lack of reliable ice thickness data close to the glacier terminus resulted in a valley under the ice that was too shallow. Figure 4 shows the difference between this new description of the bed topography and the previous data sets. We observe (Figure 4c) that the inclusion of OMG data does not change the general pattern of the bed topography (i.e., the bed features in Bedmachine and in this study are the same), but the inclusion of OMG introduces an offset in the bed elevation. The initial MC bed from Bedmachine was about 150 m higher, most likely because of errors in the surface mass balance and/or the ice thinning rate near the glacier front.

Figures 3d–f and 4d–f show the same maps for South Hayes, a marine-terminating ice stream about 250 km south of Savissuaq Gletscher. South Hayes (74.8°N, 56.7°W) is one of the ice streams that branches off from Hayes Gletscher, a major outlet glacier that flows over a deep trough (1,000 m below sea level). In the map from Bamber et al. (2013), the fjord is above sea level 10 km away from the glacier terminus, which makes South Hayes appear to be a land-terminating glacier. The bed topography under the glacier itself rises near the front and reaches sea level at its terminus. MC, on the other hand, detects a pattern consistent with the ice velocity that depicts a glacier front about 500 m below sea level and two distinct branches that merge 5 km upstream of the glacier terminus (Figure 3e). Without including OMG data, MC already provides a bed topography that is in close agreement with OMG bathymetry at the glacier front (Figures 3e,f and 4d). This is not specific to South Hayes, the previous example (Savissuaq Gletscher) being one of the few exceptions. We find that MC-derived ice front depths are
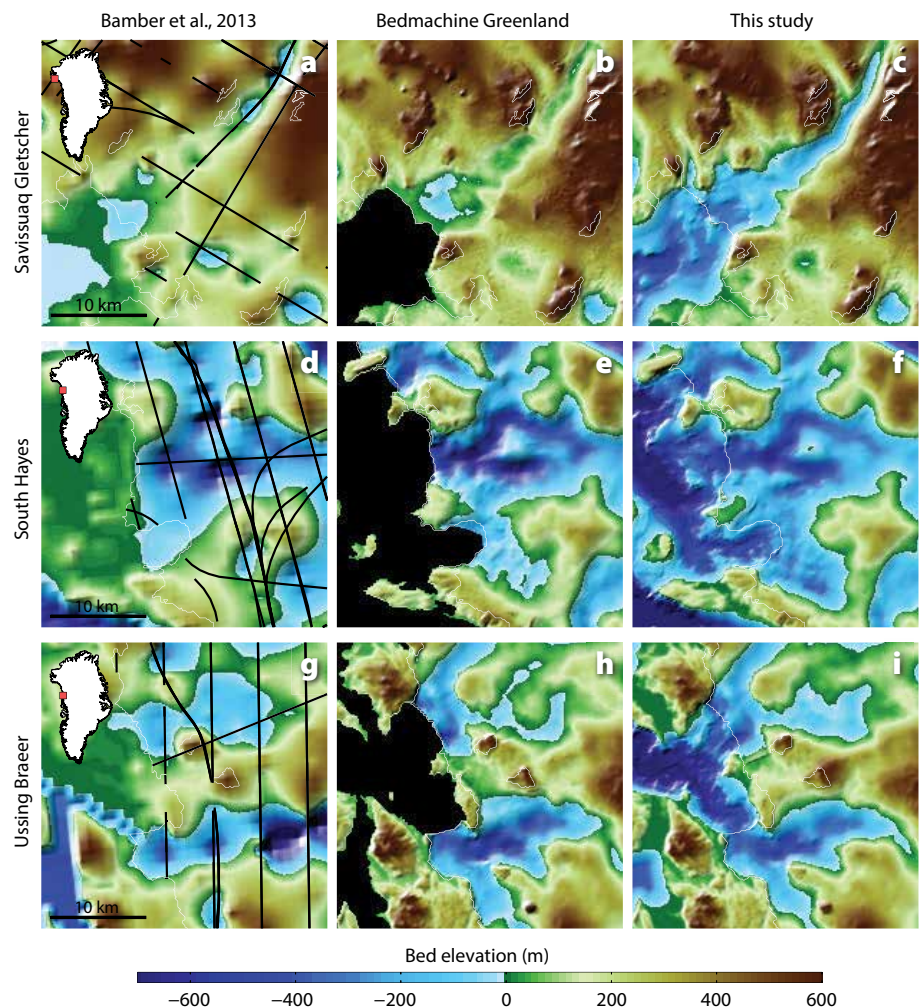
FIGURE 3. Bed elevation beneath (a–c) Savissuaq Gletscher, (d–f) South Hayes, and (g–i) Ussing Bræer from Bamber et al. (2013) in (a,d,g), Morlighem et al. (2014) using mass conservation in (b,e,h), and including bathymetry data in (c, f, i) color coded between −700 m and +600 m, with areas below sea level in blue. The white lines delineate the limit of land ice.

generally within 100 m of OMG bathymetry data, which gives some confidence in the reliability of MC even in regions where the glacier termini are poorly constrained. The inclusion of OMG data (Figure 3f) makes it possible to evaluate the MC-derived bed, correct the remaining error near the ice front, and provide a more accurate mapping of bed topography. The valley 5 km south of the main ice stream in Figure 3f appears about 100 m deeper than what MC inferred originally, even though the general shape of the bed is conserved (Figure 4f).

Finally, Ussing Bræer and Ussing Bræer N (Figures 3g–i and 4g–i) are located ~100 km south of Hayes (73.9°N, 55.7°W). Their ice fronts are 5 km and 8 km wide, respectively. In the previous mapping from Bamber et al. (2013) and IBCAO, the fjord depth is mostly flat above sea level, with the exception of a narrow fjord along Ussing Bræer that was introduced manually. The bed topography of the glaciers shows bumps between flight lines that are typical artifacts of Kriging and not realistic. Without accounting for bathymetry data, MC is able to correctly capture the general shape of the bed topography with a correct depth of ~600 m and ~400 m below sea level at the glacier fronts (Figure 3h).

Including OMG bathymetry data (Figure 3i) yields a slightly deeper valley (Figure 4f) and shows excellent agreement with the bathymetry data collected near the glacier front. Our mapping suggests that the Ussing Bræer bed deepens inland. We can posit that if its ice front retreats by 3 km, Ussing Bræer will start a phase of fast retreat of about 8 km along retrograde bed.

Applying a similar technique to other ice streams in the northwest (e.g., Steenstrup Gletscher, Rink Gletscher, Yngvar Nielsen Bræ), we find that MC-inferred depths at glacier termini before integrating OMG data were,
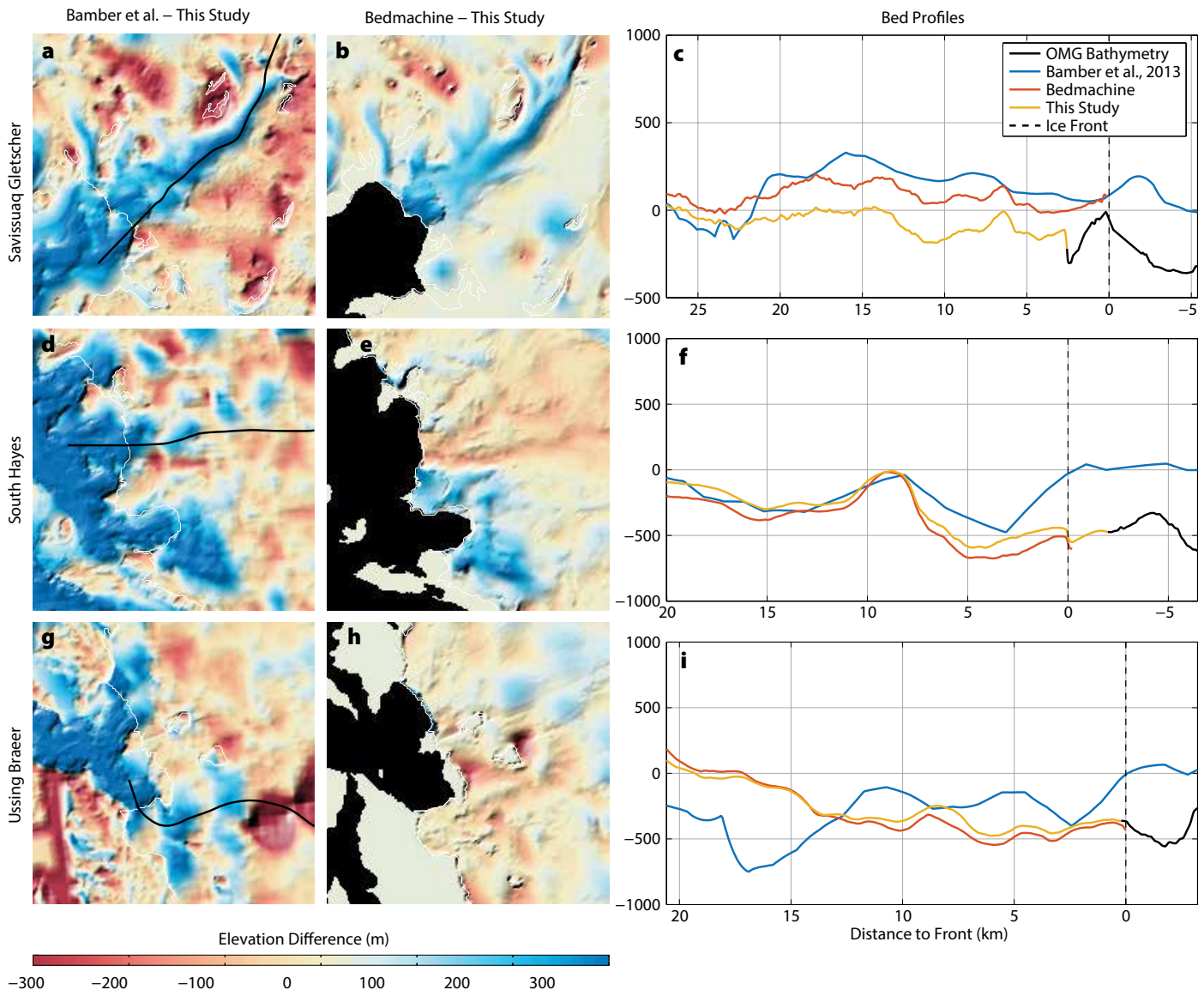
FIGURE 4. Difference between Bamber et al. (2013) (a,d,g), Morlighem et al. (2014) (b,e,h), and this study over (a–c) Savissuaq Gletscher, South Hayes (d–f), and Ussing Bræer (g–i). The right panels show the three bed profiles and OMG bathymetry data along the flow lines shown in black on the left panels.

as mentioned above, already in reasonable agreement with newly collected bathymetry data; this was despite the lack of ice thickness data near glacier termini and potential large errors in ice thinning rates and surface mass balance. Integrating OMG data reduces the error in the vicinity of the ice front and in the region directly upstream of the ice front, and makes the mapping more robust and seamless as it is more constrained in regions that rarely have reliable radar ice thickness data. To illustrate that improvement, Figure 5 shows the bed topography from Bamber et al. (2013) and from MC together with OMG in the northern part of Northwest Greenland. OMG data reveal unique features in the bathymetry, such as deep fjords (more than 1,000 m below sea level in places) that extend below the ice sheets for tens of kilometers according to MC, free of Kriging artifacts (e.g., "string of beads" along flight lines clearly visible on Figure 5a). Our new data set (Figure 5b) provides continuous mapping of the bathymetry and the subglacial bed topography.

The second phase of this work consists of "stitching" the MC bed with OMG bathymetry data in order to provide a complete and seamless map of bed topography that covers the seafloor, the fjords, ice-free land, and the topography under grounded ice. Figure 6b shows our new bed for comparison with the bed from Bamber et al. (2013), depicted in Figure 6a, over the northwest coast of Greenland from 73°N to 76°N. In the Figure 6a bed topography, glacier termini are above or close to sea level for many of the ice streams and are missing important features like ridges and valleys that play critical roles in ice dynamics. Our OMG-MC mapping (Figure 6b) provides seamless transitions at the glacier termini and is consistent with ice physics because it relies on the conservation of mass (Seroussi et al., 2011; Aschwanden et al., 2016).

While the bathymetry of IBCAOv3 is shallow and flat, OMG data show a dozen narrow (5 km) and deep (>800 m below sea level) fjords that coincide with the position of current ice streams at the ice boundary. These networks of deep paleofjords, revealed by OMG for the first time, are of glacial origin (i.e., generated by long-term—hundreds of thousands of years—glacial erosion of the bed; Kessler et al., 2008). Greenland ice streams advance and retreat during glacial cycles, sometimes reaching the continental shelf break, which results in significant erosion of the bedrock still visible today. The combination of OMG and MC gives an unprecedented picture of present and past glacial landscapes.

More importantly, this mapping provides the first complete and accurate description of the glacier bed and bathymetry of this region. Ocean circulation models could not be used in these regions previously, as the bathymetry was unknown. This new map, together with OMG temperature and salinity data from CTDs, opens the door to modeling ocean circulation in the entire fjord system in three dimensions, making it possible to better understand the vertical structure of ocean waters and its temporal variability. Ultimately, these new maps will make projections of the ice sheet contribution to sea level rise over the next centuries more reliable. As OMG expands its coverage, we will update the MC maps over grounded ice, extend our mapping to include the
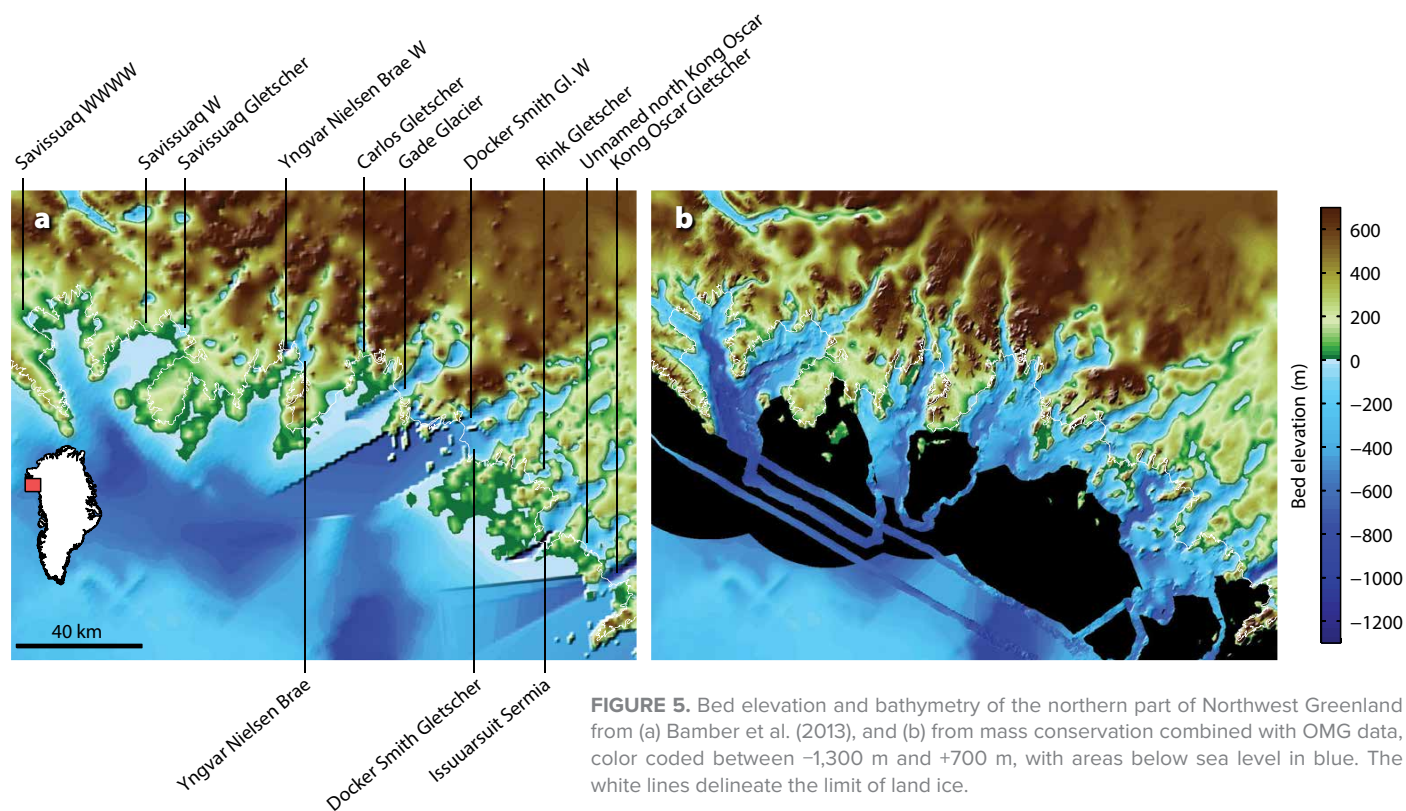
FIGURE 5. Bed elevation and bathymetry of the northern part of Northwest Greenland from (a) Bamber et al. (2013), and (b) from mass conservation combined with OMG data, color coded between –1,300 m and +700 m, with areas below sea level in blue. The white lines delineate the limit of land ice.
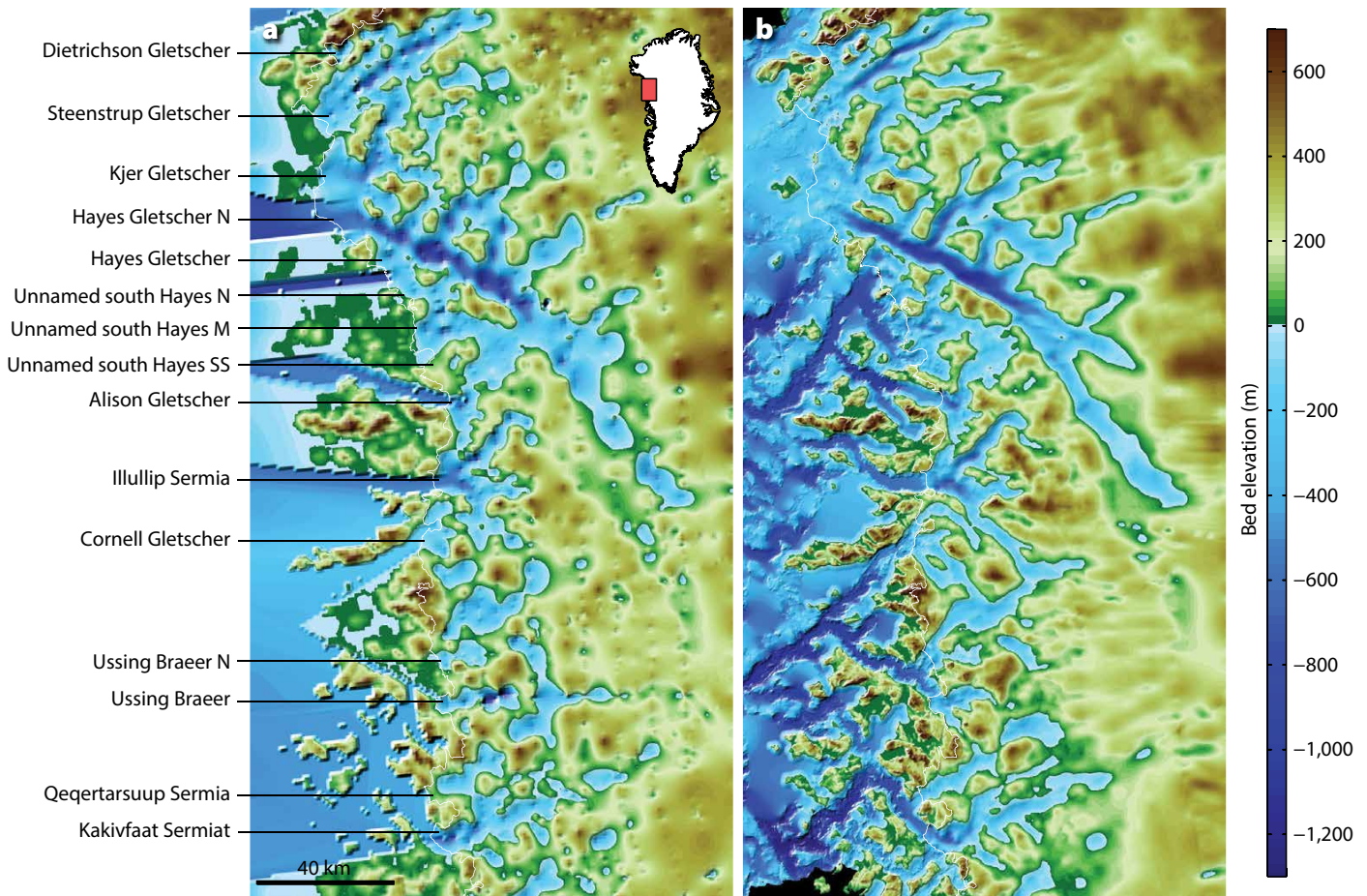
FIGURE 6. Bed elevation and bathymetry of Northwest Greenland from Bamber et al. (2013) (a) and from mass conservation combined with OMG data (b) color coded between −1,300 m and +700 m, with areas below sea level in blue. The white lines delineate the limit of land ice.

entire periphery of the Greenland Ice Sheet, and release the final product to the community.

CONCLUSIONS

We combine here for the first time mass conservation glacier bed mapping and newly collected bathymetry data from OMG to evaluate and improve descriptions of bed topography under grounded ice near glacier termini, where it matters most for improving the reliability of ice sheet models. Ice thickness and bed topography are routinely measured by airborne sounding radars, but this technique remains challenging to use near the coast. MC provides reasonable bed elevation estimates over the periphery of the ice sheet, but remains poorly constrained by radar data. OMG data are transforming our knowledge of bathymetry, and the addition of OMG bathymetry data near

the ice fronts makes MC-derived bed topography more reliable in the vicinity of these fronts. Assembling OMG bathymetry and MC bed topography makes it possible to construct a complete, seamless, and highly reliable description of the topography of the ice sheet and the entire fjord system. We expect projections of sea level rise to be vastly improved with these new maps, as they represent a major improvement over existing data sets. This new bed topography map will be available in the next version of Bedmachine Greenland at the National Snow and Ice Data Center. 🄫

REFERENCES

Aschwanden, A., M. Fahnestock, and M. Truffer. 2016. Complex Greenland outlet glacier flow captured. *Nature Communications* 7:1–8, https://doi.org/10.1038/ncomms10524.

Bamber, J.L., J.A. Griggs, R.T.W.L. Hurkmans, J.A. Dowdeswell, S.P. Gogineni, I. Howat, J. Mouginot, J. Paden, S. Palmer, E. Rignot, and

D. Steinhage. 2013. A new bed elevation dataset for Greenland. *Cryosphere* 7:499–510, https://doi.org/10.5194/tc-7-499-2013.

Enderlin, E.M., I.M. Howat, S. Jeong, M.-J. Noh, J.H. van Angelen, and M.R. van den Broeke. 2014. An improved mass budget for the Greenland ice sheet. *Geophysical Research Letters* 41(3):866–872, https://doi.org/10.1002/2013GL059010.

Ettema, J., M.R. van den Broeke, E. van Meijgaard, W.J. van de Berg, J.L. Bamber, J.E. Box, and R.C. Bales. 2009. Higher surface mass balance of the Greenland Ice Sheet revealed by high-resolution climate modeling. *Geophysical Research Letters* 36:1–5, https://doi.org/10.1029/2009GL038110.

Evans, S., and G. de Q. Robin. 1966. Glacier depth-sounding from air. *Nature* 210:883–885, https://doi.org/10.1038/210883a0.

Gogineni, S., T. Chuah, C. Allen, K. Jezek, and R. Moore. 1998. An improved coherent radar depth sounder. *Journal of Glaciology* 44(148):659–669.

Gudmundsson, G.H., J. Krug, G. Durand, L. Favier, and O. Gagliardini. 2012. The stability of grounding lines on retrograde slopes. *Cryosphere* 6(6):1,497–1,505, https://doi.org/10.5194/tc-6-1497-2012.

Holt, J., M. Peters, S. Kempf, D. Morse, and D. Blankenship. 2006. Echo source discrimination in single-pass airborne radar sounding data from the Dry Valleys, Antarctica: Implications for orbital sounding of Mars. *Journal of Geophysical Research* 111(E6):1–13, https://doi.org/10.1029/2005JE002525.

Howat, I.M., I. Joughin, and T.A. Scambos. 2007. Rapid changes in ice discharge from Greenland outlet glaciers. *Science* 315:1,559–1,561, https://doi.org/10.1126/science.1138478.

Howat, I.M., A. Negrete, and B.E. Smith. 2014. The Greenland Ice Mapping Project (GIMP) land classification and surface elevation datasets. *Cryosphere* 8(4):1,509–1,518, https://doi.org/10.5194/tc-8-1509-2014.

Jakobsson, M., L. Mayer, B. Coakley, J.A. Dowdeswell, S. Forbes, B. Fridman, H. Hodnesdal, R. Noormets, R. Pedersen, M. Rebesco, and others. 2012. The International Bathymetric Chart of the Arctic Ocean (IBCAO) Version 3.0. *Geophysical Research Letters* 39:1–6, https://doi.org/10.1029/2012GL052219.

Joughin, I., R.B. Alley, and D.M. Holland. 2012. Ice-sheet response to oceanic forcing. *Science* 338:1,172–1,176, https://doi.org/10.1126/science.1226481.

Kessler, M.A., R.S. Anderson, and J.P. Briner. 2008. Fjord insertion into continental margins driven by topographic steering of ice. *Nature Geoscience* 1(6):365–369, https://doi.org/10.1038/ngeo201.

Moon, T., I. Joughin, and B. Smith. 2015. Seasonal to multiyear variability of glacier surface velocity, terminus position, and sea ice/ice melange in northwest Greenland. *Journal of Geophysical Research* 120(5):818–833, https://doi.org/10.1002/2015JF003494.

Morlighem, M., J. Bondzio, H. Seroussi, E. Rignot, E. Larour, A. Humbert, and S.-A. Rebuffi. 2016. Modeling of Store Gletscher's calving dynamics, West Greenland, in response to ocean thermal forcing. *Geophysical Research Letters* 43(6):2,659–2,666, https://doi.org/10.1002/2016GL067695.

Morlighem, M., E. Rignot, J. Mouginot, H. Seroussi, and E. Larour. 2014. Deeply incised submarine glacial valleys beneath the Greenland Ice Sheet. *Nature Geoscience* 7(6):418–422, https://doi.org/10.1038/ngeo2167.

Morlighem, M., E. Rignot, J. Mouginot, X. Wu, H. Seroussi, E. Larour, and J. Paden. 2013. High-resolution bed topography mapping of Russell Glacier, Greenland, inferred from Operation IceBridge data. *Journal of Glaciology* 59(218):1,015–1,023, https://doi.org/10.3189/2013JoG12J235.

Morlighem, M., E. Rignot, H. Seroussi, E. Larour, H. Ben Dhia, and D. Aubry. 2011. A mass conservation approach for mapping glacier ice thickness. *Geophysical Research Letters* 38, L19503, https://doi.org/10.1029/2011GL048659.

Mouginot, J., E. Rignot, B. Scheuchl, I. Fenty, A. Khazendar, M. Morlighem, A. Buzzi, and J. Paden. 2015. Fast retreat of Zachariæ Isstrøm, Northeast Greenland. *Science* 350:1,357–1,361, https://doi.org/10.1126/science.aac7111.

OMG Mission. 2016a. *Bathymetry (sea floor depth) data from the ship-based bathymetry survey. Ver. 0.1.* OMG SDS, CA, https://doi.org/10.5067/OMGEV-BTYSS.

OMG Mission. 2016b. *Glacier elevation data from the GLISTIN-A campaigns. Ver. 0.1.* OMG SDS, CA, https://doi.org/10.5067/OMGEV-ICEGA.

Pattyn, F., L. Perichon, G. Durand, L. Favier, O. Gagliardini, R.C.A. Hindmarsh, T. Zwinger, T. Albrecht, C. Torsten, S. Cornford, and others. 2013. Grounding-line migration in plan-view marine ice-sheet models: Results of the ice2sea MISMIP3d intercomparison. *Journal of Glaciology* 59(215):410–422, https://doi.org/10.3189/2013JoG12J129.

Post, A. 1975. Preliminary hydrography and historic terminal changes of Columbia Glacier, Alaska. Hydrologic Atlas 559, US Geological Survey, https://pubs.er.usgs.gov/publication/ha559.

Rignot, E., I. Fenty, Y. Xu, C. Cai, and C. Kemp. 2015. Undercutting of marine-terminating glaciers in West Greenland. *Geophysical Research Letters* 42(14):5,909–5,917, https://doi.org/10.1002/2015GL064236.

Rignot, E., and J. Mouginot. 2012. Ice flow in Greenland for the International Polar Year 2008–2009. *Geophysical Research Letters* 39, L11501, https://doi.org/10.1029/2012GL051634.

Rignot, E., I. Velicogna, M. van den Broeke, A. Monaghan, and J. Lenaerts. 2011. Acceleration of the contribution of the Greenland and Antarctic ice sheets to sea level rise. *Geophysical Research Letters* 38:1–5, https://doi.org/10.1029/2011GL046583.

Schenk, T., and B. Csatho. 2012. A new methodology for detecting ice sheet surface elevation changes from laser altimetry data. *IEEE Transactions on Geoscience and Remote Sensing* 50(9):3,302–3,316, https://doi.org/10.1109/TGRS.2011.2182357.

Schoof, C. 2007. Ice sheet grounding line dynamics: Steady states, stability, and hysteresis. *Journal of Geophysical Research* 112, F03S28, https://doi.org/10.1029/2006JF000664.

Seroussi, H., M. Morlighem, E. Rignot, E. Larour, D. Aubry, H. Ben Dhia, and S.S. Kristensen. 2011. Ice flux divergence anomalies on 79north Glacier, Greenland. *Geophysical Research Letters* 38, L09501, https://doi.org/10.1029/2011GL047338.

Shepherd, A., E.R. Ivins, Geruo A., V.R. Barletta, M.J. Bentley, S. Bettedpur, K.H. Briggs, D.H. Bromwich, R. Forsberg, N. Galin, and others. 2012. A reconciled estimate of ice-sheet mass balance. *Science* 338:1,183–1,189, https://doi.org/10.1126/science.1228102.

Velicogna, I., T.C. Sutterley, and M.R. van den Broeke. 2014. Regional acceleration in ice mass loss from Greenland and Antarctica using GRACE time-variable gravity data. *Geophysical Research Letters* 41(22):8,130–8,137, https://doi.org/10.1002/2014GL061052.

Weertman, J. 1974. Stability of the junction of an ice sheet and an ice shelf. *Journal of Glaciology* 13(67):3–11.

AUTHORS

Mathieu Morlighem (mathieu.morlighem@uci.edu) is Assistant Professor, Department of Earth System Science, University of California, Irvine, CA, USA. **Eric Rignot** is Chancellor Professor, Department of Earth System Science, University of California, Irvine, CA, USA, and Principal Scientist, Radar Science and Engineering Section, Jet Propulsion Laboratory, California Institute of Technology, Pasadena, CA, USA. **Josh K. Willis** is Project Scientist, Jet Propulsion Laboratory, California Institute of Technology, Pasadena, CA, USA.